

# Efficient Fabry-Perot Open Resonator Analysis by the use of a Scattering Matrix Method

Malgorzata Warecka, Sebastian Dziedziewicz,  
Piotr Kowalczyk, Rafal Lech

*Department of Microwave and Antenna Engineering,  
Faculty of Electronics, Telecommunications and Informatics  
Gdansk University of Technology,  
Narutowicza 11/12, 80-233 Gdansk, Poland,  
e-mail: malgorzata.warecka@pg.edu.pl*

Piotr Czekala, Bartlomiej Salski, Pawel Kopyt

*Warsaw University of Technology,  
Institute of Radioelectronics and Multimedia Technology,  
Nowowiejska 15/19, 00-665 Warsaw, Poland*

**Abstract**—In this paper a comparative study of the computational efficiency of two modeling methods applied to the analysis of the plano- and double-concave Fabry-Perot open resonators is presented. In both numerical approaches, a scattering matrix method was applied, which allows splitting the analysis of the resonator into several sections, including the one with a spherical mirror, which requires the largest computing resources. Two modeling techniques were utilized to evaluate the scattering matrix of the spherical mirror, namely, the finite element method and free-space Green's function method. Resonant frequencies and the corresponding field distributions of the selected Gaussian modes were calculated and compared. Good agreement between the methods was achieved; however, the Green's function method has occurred to be more computationally efficient.

**Index Terms**—Fabry-Perot open resonator, finite element method, Green's function, resonant frequency

## I. INTRODUCTION

A Fabry-Perot open resonator (FPOR) is applicable in material characterization [1]–[5]. There are two common configurations of the FPOR, namely, plano-concave [6] and double-concave [7], as illustrated in Fig. 1. Both FPOR geometries are unique, as compared to other types of the resonators, due to a very high Q-factor of Gaussian modes, which are evenly distributed in the frequency spectrum. Consequently, it allows for broadband and highly accurate electromagnetic characterization of low-loss dielectric sheets. However, due to large electromagnetic dimensions, simulations of the FPOR can be very challenging. The discrete full-wave electromagnetic analysis with such methods as a finite-difference time-domain (FDTD) method or a finite element method (FEM) is expensive in terms of memory and computation time [8]–[12]. Moreover, numerical dispersion may significantly alter the parameters of tested materials.

Recently, a scattering matrix method (SMM) that substantially alleviates the aforementioned challenges in the EM

This work has received financial support from the following sources: the ministry subsidy for research for Gdansk University of Technology, project POIR.04.04.00-00-IDC3/16 carried out within the TEAM-TECH programme operated by the Foundation for Polish Science co-financed by the European Union under the European Regional Development Fund, Smart Growth Operational Programme 2014–2020, and Warsaw University of Technology within the internal project “Light-matter interaction of dielectric micro-resonators with microwave photons in a Fabry-Perot open resonator”.

modeling of the FPOR has been developed [7]. Although the FPOR is an open structure, fundamental Gaussian  $TEM_{0,0,q}$  modes do not radiate as they are concentrated around the resonator's revolution axis. Consequently, insertion of the FPOR into a cylindrical waveguide, for modelling purposes only, does not affect resonance frequencies of these modes. The advantage of such approach is, however, that EM fields can be represented as a discrete sum of waveguide modes. In addition to that, the FPOR is divided in the SMM into three non-resonant sections: two mirrors and a cylindrical waveguide section where the sample can be present. For each section, a multimode scattering matrix is calculated, and all the sections are connected into a cascade to obtain the characteristic equation, the solution of which brings resonance frequencies of the FPOR. The multimode scattering matrix of the waveguide section and that of a planar mirror can be obtained analytically, whereas a spherical mirror has to be computed numerically.

This paper is focused on the accurate determination of the scattering matrix of the spherical mirror, which is numerically the most challenging part of the SMM, so it should be computationally efficient. Therefore, two different calculation methods are utilized and the results are compared. The first one is FEM which is the most general, however, its efficiency is low. The second one involves the calculation of Green's function in free space, which allows for obtaining the results much faster than the utilization of waveguide Green's function. Even though the structure is modeled as a closed one, it is possible to utilize Green's function method in free space (GFM-FS) as the waveguide modes are not taken into consideration. The only drawback to this approach is the small radiation effect, which results in the existence of imaginary part of the resonant frequency. In order to validate the usage of GFM-FS approach several Gaussian modes were investigated for resonators with different radii of mirrors.

## II. NUMERICAL METHODS

The investigated resonator structure is divided in the analysis into three sections: two mirrors and a waveguide junction (optionally with the analyzed sample). Let us denote the

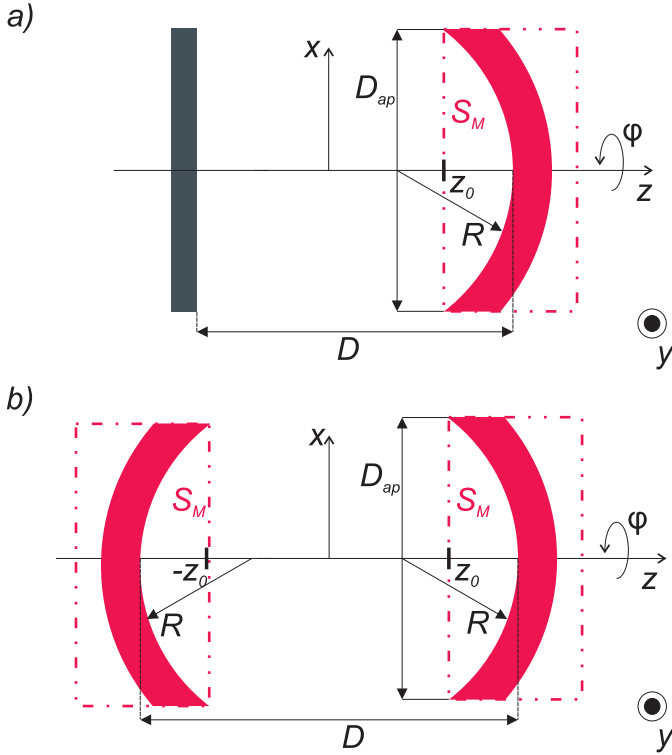


Fig. 1. a) Plano- and b) double-concave Fabry-Perot open resonators.

scattering matrix of the cascade connection of one mirror and a waveguide junction at  $z = z_0$  by  $\mathbf{S}_P$ , and the scattering matrix of spherical mirror at  $z = z_0$  by  $\mathbf{S}_M$ . It is worth noting that in the case of plano-concave FPOR the  $\mathbf{S}_P$  matrix can be obtained analytically. The cascade connection of this components leads to the following formula [7]:

$$(\mathbf{I} - \mathbf{S}_P(f_r)\mathbf{S}_M(f_r)) \mathbf{a} = 0 \quad (1)$$

where  $f_r$  is the resonant frequency and  $\mathbf{a}$  represents the vector of investigated mode amplitudes. In general, the problem can be solved by finding zeroes of the characteristic equation:

$$\det(\mathbf{I} - \mathbf{S}_P(f_r)\mathbf{S}_M(f_r)) = 0 \quad (2)$$

In this section, two methods of obtaining the scattering matrix of the spherical mirror are presented.

#### A. Scattering matrix $\mathbf{S}_M$ with the use of GFM-FS

This approach involves Green's function in free space to describe the scattering matrix of the mirror, hence some radiation losses are introduced. In order to calculate scattering matrix of the spherical mirror, firstly, the surface of a mirror has to be discretized into cylindrical cells, as shown in Fig. 2 with unit vectors,  $\hat{n}$ , normal to the mirror's surface within each cell. The mirror is, subsequently, illuminated with TE and TM modes normalized by the following coefficient (square root of power):

$$S_{(m,n)}^{sq} = \sqrt{\left| \iint_S (\vec{E}_{t,(m,n)} \times \vec{H}_{t,(m,n)}^*) \rho d\rho d\varphi \right|} \quad (3)$$

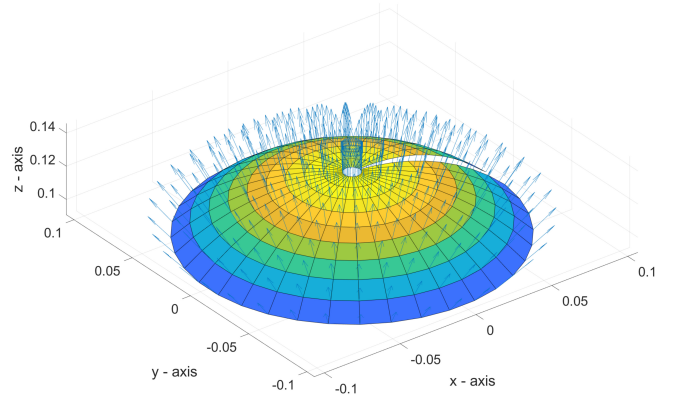


Fig. 2. Cylindrical discretization of a spherical mirror with normal surface vectors (blue arrows).

where  $S$  represents a port defined in a transverse  $xy$ -plane,  $m$  is an azimuthal mode order,  $n$  is a radial mode order and  $t$  in the subscripts denotes transverse field components.

Subsequently, the following relation is used to compute an equivalent electric surface current distribution at the mirror's surface:

$$\vec{J}_s = \hat{n} \times 2\vec{H}_{(m,n)} \quad (4)$$

furthermore the magnetic field of the scattered wave is calculated with the use of near-field scattering equations [13]:

$$\vec{H}_{x,scat}(x, y, z_0) = \iint_A [(z_0 - z')J_{s,y} - (y - y')J_{s,z}] \frac{1 + jkR}{4\pi R^3} e^{-jkR} ds' \quad (5)$$

$$\vec{H}_{y,scat}(x, y, z_0) = \iint_A [(x - x')J_{s,z} - (z_0 - z')J_{s,x}] \frac{1 + jkR}{4\pi R^3} e^{-jkR} ds' \quad (6)$$

where  $A$  is a mirror surface and the primed coordinates represent the mirror's surface and the unprimed coordinates represent the reference plane at  $z = z_0$ . It may be noticed that in above equation GFM-FS has been used. Due to that computational effort has been reduced, however, it introduces numerical losses which has to be taken into account as an imaginary part of frequency.

Once the scattered field at given reference plane has been computed, the scattering coefficients (from the  $i$ -th to the  $j$ -th mode) may be obtained using the following relation [14]:

$$S_{j,i} = \iint_S (\vec{E}_{t,inc,i} \times \vec{H}_{t,scat,j}^*) \rho d\rho d\varphi \quad (7)$$

#### B. Scattering matrix $\mathbf{S}_M$ with the use of FEM

The scattering matrix of the spherical mirror with the use of FEM is obtained from the generalized impedance matrix (GIM). GIM requires finding the relation between the electric and magnetic fields at the port of the mirror (in the reference plane  $z_0$ ). We assume that the fields at this port can be

expressed as a sum of the modal basis functions of a circular waveguide  $\vec{e}_{\xi,q}^{(\cdot),P}$  and  $\vec{h}_{\xi,q}^{(\cdot),P}$  defined in [15] for  $\xi = \{t, \varphi\}$ :

$$\vec{E}_{\xi} = \sum_{q=1}^Q (V_q^{TE} \vec{e}_{\xi,q}^{TE} + V_q^{TM} \vec{e}_{\xi,q}^{TM}), \quad (8)$$

$$\vec{H}_{\xi} = \sum_{q=1}^Q (I_q^{TE} \vec{h}_{\xi,q}^{TE} + I_q^{TM} \vec{h}_{\xi,q}^{TM}), \quad (9)$$

where  $Q$  is a number of modes taken into account in the analysis. The relation between above coefficients is represented by GIM as follows:

$$\mathbf{V} = \mathbf{Z}\mathbf{I}. \quad (10)$$

where  $\mathbf{V} = [V_1^{TE}, \dots, V_Q^{TE}, V_1^{TM}, \dots, V_Q^{TM}]^T$  and  $\mathbf{I} = [I_1^{TE}, \dots, I_Q^{TE}, I_1^{TM}, \dots, I_Q^{TM}]^T$ . The algorithm for obtaining GIM has been comprehensively described in [15], [16]. It is worth to mention that to reduce the number of elements, the Body-Of-Revolution approach was incorporated. Once the GIM is calculated, the scattering matrix can be determined using the formula:

$$\mathbf{S}_M = (\mathbf{Z} + \mathbf{U})^{-1}(\mathbf{Z} - \mathbf{U}) \quad (11)$$

where  $\mathbf{U}$  is the unit matrix.

### III. NUMERICAL RESULTS

Numerical analysis considers the PC FPOR with dimensions  $D = 100$  mm and  $D_{ap} = 200$  mm for different radii  $R$  of the spherical mirror from 120 mm to 180 mm. The resonant frequencies  $f_r$  of a few Gaussian modes  $TEM_{0,0,q}$  and the corresponding eigenvectors representing the field distribution in the resonant structure were calculated. The scattering matrix  $\mathbf{S}_M$  of spherical mirror was obtained with the use of FEM and GFM-FS. The mesh utilized in FEM involved 75 – 100 thousand of elements (second order and curvilinear) depending on  $R$ . In the GFM-FS the angular step  $\Delta\varphi$  was equal to  $5^\circ$  and the radial step  $\Delta\varrho$  was equal to 1.0 mm.

In table I the resonant frequencies of Gaussian modes are collected. As can be seen by comparing the results the relative error between the investigated models is in the order of 0.01 %. The imaginary part of  $f_r$  obtained from GFM-FS is 3 orders of magnitude smaller than the real part.

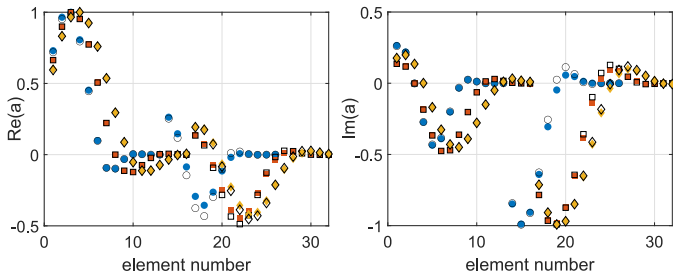


Fig. 3. The eigenvectors of Gaussian modes  $TEM_{0,0,14}$  – circles,  $TEM_{0,0,24}$  – squares and  $TEM_{0,0,33}$  – diamonds for  $R = 120$  mm; FEM – contour and GFM-FS – filled

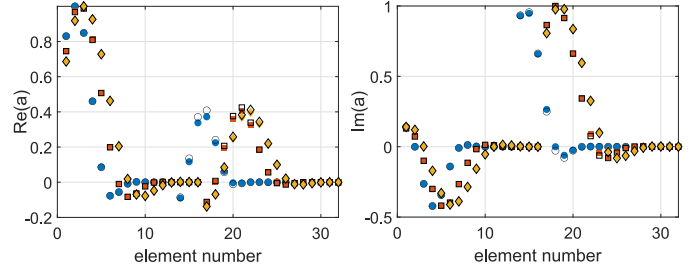


Fig. 4. The eigenvectors of Gaussian modes  $TEM_{0,0,14}$  – circles,  $TEM_{0,0,24}$  – squares and  $TEM_{0,0,33}$  – diamonds for  $R = 150$  mm; FEM – contour and GFM-FS – filled

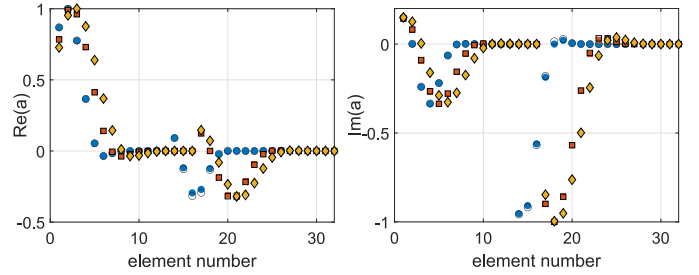


Fig. 5. The eigenvectors of Gaussian modes  $TEM_{0,0,14}$  – circles,  $TEM_{0,0,24}$  – squares and  $TEM_{0,0,33}$  – diamonds for  $R = 180$  mm; FEM – contour and GFM-FS – filled

In Figs. 3 – 5 the eigenvectors of the Gaussian modes  $TEM_{0,0,14}$ ,  $TEM_{0,0,24}$  and  $TEM_{0,0,33}$  for different radii of spherical mirror are illustrated. First 16 elements correspond to TE modes while the elements from 17 to 32 – to TM modes. The obtained results are in good agreement. However, as expected, the accuracy of the eigenvectors evaluation (field distribution) is lower than the eigenvalues (resonant frequency).

TABLE I  
RESONANT FREQUENCY OF  $TEM_{0,0,q}$  MODES

$q$	$R$ [mm]	FEM	GFM-FS		relative error [%]
		$\text{Re}(f_r)$ [GHz]	$\text{Re}(f_r)$ [GHz]	$\text{Im}(f_r)$ [MHz]	
14	120	21.532	21.535	10.454	0.0151
	130	21.494	21.497	7.819	0.0161
	140	21.464	21.467	6.251	0.0158
	150	21.439	21.443	5.195	0.0151
	160	21.419	21.422	4.433	0.0143
	170	21.401	21.404	3.854	0.0136
	180	21.385	21.388	3.401	0.0129
24	120	36.523	36.525	5.760	0.0060
	130	36.484	36.486	4.290	0.0059
	140	36.454	36.456	3.418	0.0057
	150	36.430	36.432	2.836	0.0053
	160	36.409	36.411	2.406	0.0050
	170	36.391	36.393	2.081	0.0047
	180	36.376	36.377	1.827	0.0045
33	120	50.014	50.015	3.927	0.0032
	130	49.975	49.977	2.902	0.0031
	140	49.945	49.947	2.294	0.0029
	150	49.921	49.922	1.884	0.0028
	160	49.900	49.901	1.587	0.0026
	170	49.882	49.883	1.362	0.0024
	180	49.866	49.868	1.186	0.0023

#### IV. CONCLUSIONS

The results of a Fabry-Perot open resonator analysis obtained from scattering matrix method involving FEM and GFM-FS were compared. Good agreement was achieved, which confirms the equivalence of both presented approaches. Since the use of GFM-FS is numerically significantly less expensive (at least several hundred times faster calculation) than FEM, its application seems to be much more efficient from a practical point of view. This aspect is particularly important in material characterization when the analysis must be performed multiple times (different frequency points).

#### REFERENCES

- [1] A. L. Cullen and P. Yu, "The accurate measurement of permittivity by means of an open resonator," *Proceedings of the Royal Society of London. A. Mathematical and Physical Sciences*, vol. 325, no. 1563, pp. 493–509, 1971.
- [2] P. Yu and A. L. Cullen, "Measurement of permittivity by means of an open resonator. i. theoretical," *Proceedings of the Royal Society of London. A. Mathematical and Physical Sciences*, vol. 380, no. 1778, pp. 49–71, 1982.
- [3] T. Karpisz, B. Salski, P. Kopyt, and J. Krupka, "Measurement of dielectrics from 20 to 50 ghz with a fabry-pérot open resonator," *IEEE Transactions on Microwave Theory and Techniques*, vol. 67, no. 5, pp. 1901–1908, 2019.
- [4] T. M. Hirvonen, P. Vainikainen, A. Lozowski, and A. V. Raisanen, "Measurement of dielectrics at 100 ghz with an open resonator connected to a network analyzer," *IEEE transactions on instrumentation and measurement*, vol. 45, no. 4, pp. 780–786, 1996.
- [5] B. Salski, J. Cuper, T. Karpisz, P. Kopyt, and J. Krupka, "Complex permittivity of common dielectrics in 20–110 ghz frequency range measured with a fabry-pérot open resonator," *Applied Physics Letters*, vol. 119, no. 5, p. 052902, 2021.
- [6] B. Salski, T. Karpisz, M. Warecka, P. Kowalczyk, P. Czekala, and P. Kopyt, "Microwave characterization of dielectric sheets in a plano-concave fabry-perot open resonator," *IEEE Transactions on Microwave Theory and Techniques*, pp. 1–11, 2022.
- [7] B. Salski, T. Karpisz, P. Kopyt, and J. Krupka, "Rigorous scattering matrix analysis of a fabry-pérot open resonator," *IEEE Transactions on Microwave Theory and Techniques*, vol. 68, no. 12, pp. 5093–5102, 2020.
- [8] J. S. Juntunen and T. D. Tsiboukis, "Reduction of numerical dispersion in fdtd method through artificial anisotropy," *IEEE Transactions on microwave Theory and Techniques*, vol. 48, no. 4, pp. 582–588, 2000.
- [9] J. B. Cole, "A high-accuracy realization of the yee algorithm using non-standard finite differences," *IEEE transactions on Microwave Theory and Techniques*, vol. 45, no. 6, pp. 991–996, 1997.
- [10] —, "High-accuracy yee algorithm based on nonstandard finite differences: new developments and verifications," *IEEE Transactions on Antennas and Propagation*, vol. 50, no. 9, pp. 1185–1191, 2002.
- [11] M. Rewiński and M. Mrozowski, "An iterative algorithm for reducing dispersion error on yee's mesh in cylindrical coordinates," *IEEE microwave and guided wave letters*, vol. 10, no. 9, pp. 353–355, 2000.
- [12] M. Warecka, G. Fotyga, P. Kowalczyk, R. Lech, M. Mrozowski, A. Pacewicz, B. Salski, and J. Krupka, "Modal fem analysis of ferrite resonant structures," *IEEE Microwave and Wireless Components Letters*, pp. 1–4, 2022.
- [13] C. A. Balanis, *Advanced engineering electromagnetics*. John Wiley & Sons, 2012.
- [14] W. K. Gwarek and M. Celuch-Marcysiak, "Wide-band s-parameter extraction from fd-td simulations for propagating and evanescent modes in inhomogeneous guides," *IEEE Transactions on Microwave Theory and Techniques*, vol. 51, no. 8, pp. 1920–1928, 2003.
- [15] M. Warecka, R. Lech, and P. Kowalczyk, "Efficient finite element analysis of axially symmetrical waveguides and waveguide discontinuities," *Trans. Microw. Theory Tech.*, vol. 67, no. 11, pp. 4291–4297, Nov. 2019.
- [16] —, "Hybrid analysis of structures composed of axially symmetric objects," *IEEE Trans. Microw. Theory Techn.*, vol. 68, no. 11, pp. 4528–4535, Nov. 2020.